

See discussions, stats, and author profiles for this publication at: <https://www.researchgate.net/publication/7704001>

Micellar Structure in Gemini Nonionic Surfactants from Small-Angle Neutron Scattering

ARTICLE *in* LANGMUIR · SEPTEMBER 2005

Impact Factor: 4.46 · DOI: 10.1021/la0467988 · Source: PubMed

CITATIONS

20

READS

36

3 AUTHORS, INCLUDING:



Gregory G Warr

University of Sydney

189 PUBLICATIONS 4,996 CITATIONS

SEE PROFILE

Micellar Structure in Gemini Nonionic Surfactants from Small-Angle Neutron Scattering

Paul A. FitzGerald,[†] Tim W. Davey,[‡] and Gregory G. Warr*

School of Chemistry F11, The University of Sydney, NSW 2006 Sydney, Australia

Received December 23, 2004. In Final Form: May 27, 2005

The size and shape of micelles formed by dimeric polyoxyethylene (nonionic gemini) surfactants having the structure $(C_{n-2}H_{2n-3}CHCH_2(OCH_2CH_2)_mOH)_2(CH_2)_6$ with alkyl and ethoxy chain lengths ranging from $n = 12$ –20 and $m = 5$ –30 have been determined using small angle neutron scattering (SANS). The surfactants are polydisperse in the hydrophilic groups but otherwise analogous to the widely studied monomeric poly(oxyethylene) alkanols. We find that longer ethoxylated chains are needed to confer solubility on the gemini surfactants and that these chains in the hydrophilic corona around the alkyl core of the micelles are reasonably well described as a homogeneous random coil in a good solvent. Spherical micelles are formed by the surfactants with the longest ethoxylated chains. Shorter chains lead first to rods and ultimately a vesicle dispersion. These solutions exhibit conventional cloud point behavior, and on warming, a sphere to rod transition can be observed. For the $n = 20$ and $m = 15$ surfactant, this shape transition is accompanied by a striking increase in viscosity at low concentration and gelation at higher concentrations.

Introduction

In recent years there has been increasing interest in dimeric (gemini) surfactants, which consist of two conventional surfactants joined by a spacer at or near the headgroup, as they exhibit much lower critical micelle concentrations (CMCs) than can be achieved by conventional surfactants. Cationic bis(quaternary ammonium) surfactants have been most extensively studied, and the dependence of their properties on systematic variation of alkyl chain length, spacer length and type, and electrolyte concentration have been described.¹ Small-angle neutron scattering has recently been employed to reveal micelle structure in a variety of gemini surfactant solutions,² and recently, an unusual nonionic gemini has been examined.³

In this work, we examine a series of very hydrophobic nonionic gemini surfactants with the structure $(C_{n-2}H_{2n-3}CHCH_2(OCH_2CH_2)_mOH)_2(CH_2)_6$, abbreviated Gem_nE_m , where m is the average number of ethylene oxide units per headgroup, shown in Figure 1. Their preparation and CMCs have been described previously.⁴ The present work is concerned with how the micelle morphology and isotropic solution structure of these gemini surfactants depend on the ethoxylation number (m) and alkyl chain length (n), concentration, and temperature and how these trends compare to conventional nonionic surfactants.

Alkyl chain lengths are varied between 12 and 20 with a fixed hexamethylene spacer. Ethoxylation was carried

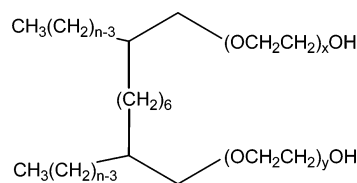


Figure 1. Generic structure of nonionic gemini surfactants, Gem_nE_m , used in this study. $m = 1/2(x + y)$ is the average degree of ethoxylation per alkyl chain.

out by ring-opening polycondensation, leading to a distribution of ethoxy chain lengths about an average $m = 5, 10, 15, 20$, or 30 .⁴ The most hydrophobic surfactants, those with the smallest headgroups, $Gem_{12}E_5$, $Gem_{14}E_5$, and $Gem_{20}E_{10}$, are all insoluble at room temperature, forming a dispersed lamellar phase (vesicles) in water, and were not investigated in this work. The remaining surfactants all have extremely low CMCs, in the range $(1.5\text{--}7) \times 10^{-7}$ M.

Self-assembly structures, and particularly systematic trends in micelle morphology, can be rationalized using the surfactant packing parameter,⁵ v/a_0l_c , where v is the volume of a surfactant hydrocarbon tail, a_0 is the effective area per headgroup, and l_c is the fully extended alkyl chain length. l_c forms an upper bound on the radius of a spherical or cylindrical micelle, or the half-thickness of a bilayer. Spherical micelles form for a packing parameter less than or equal to one-third, rodlike micelles form for a packing parameter between one-third and one-half, and bilayers form for a packing parameter between one-half and one.

For conventional or gemini nonionic surfactants, both l_c and v increase linearly with alkyl chain length,⁶ and changes in degree of ethoxylation alter a_0 . Thus, as ethoxylation number, and hence a_0 , is increased, the micelle morphology is expected to change toward higher curvature: from planar to rodlike to spherical. Increasing alkyl chain length causes a slight decrease in aggregate curvature.

* To whom correspondence should be addressed. E-mail: g.warr@chem.usyd.edu.au.

[†] Current address: Chemistry, School of Environmental and Life Sciences, The University of Newcastle, Callaghan, NSW 2308 Australia.

[‡] Current address: Dulux Australia Research and Development, Clayton, Vic., 3168 Australia.

(1) Zana, R. *Adv. Colloid Interface Sci.* **2002**, *97*, 205. Zana, R.; Benraou, M.; Rueff, R. *Langmuir* **1991**, *7*, 1072.

(2) Wang, X.; Wang, J.; Yan, H.; Li, P.; Thomas, R. K. *Langmuir* **2004**, *19*, 53. Sharma, V.; Borse, M.; Aswal, V. K.; Pokhriyal, N. K.; Joshi, J. V.; Goyal, P. S.; Devi, S. *J. Colloid Interface Sci.* **2004**, *277*, 450–455. Alami, E.; Abrahmese'n-Alami, S.; Eastoe, J.; Heenan, R. K. *Langmuir* **2003**, *19*, 18–23.

(3) Nieh, M.-P.; Sanat K.; Kumar, S. K.; Fernando, R. H.; Colby, R. H.; Katsaras, J. *Langmuir* **2004**, *20*, 9061–9068.

(4) FitzGerald, P. A.; Carr, M. W.; Davey, T. W.; Serelis, A. K.; Such, C. H.; Warr, G. G. *J. Colloid Interface Sci.* **2004**, *275*, 649–658.

(5) Israelachvili, J. N.; Mitchell, J. D.; Ninham, B. W. *J. Chem. Soc., Faraday Trans. 2* **1976**, *72*, 1525–1568.

(6) Tanford, C. *The Hydrophobic Effect*, 2nd ed.; Wiley: New York, 1980.

As the temperature is increased toward the cloud temperature, many conventional nonionic surfactants exhibit micellar growth.^{7–9} The exact nature of micelle behavior in this region has not been fully explained but it is widely believed that as the cloud temperature is approached the polyoxyethylene headgroups begin to dehydrate,¹⁰ which decreases the area occupied, a_0 . This leads to a sphere-to-rod transition, and some have proposed a rod to branched-rod or network transition near the cloud temperature.^{11,12} Because of their high hydrophobicity, these nonionic micelles display some unusual viscosity behavior accompanying the morphology change as the cloud point is approached.

Materials and Methods

The nonionic gemini surfactants, Gem_nE_m , were synthesized as described previously⁴ with the structure $(\text{C}_{n-2}\text{H}_{2n-3}\text{CHCH}_2(\text{OCH}_2\text{CH}_2)_m\text{OH})_2(\text{CH}_2)_6$. Ethoxylation is carried out as a polycondensation, leading to a distribution of hydrophilic ethoxy chain lengths about a mean, m , per alkyl tail (see Figure 1). The surfactants investigated here are $\text{Gem}_{12}\text{E}_{10}$, $\text{Gem}_{12}\text{E}_{15}$, $\text{Gem}_{14}\text{E}_{10}$, $\text{Gem}_{14}\text{E}_{15}$, $\text{Gem}_{20}\text{E}_{15}$, $\text{Gem}_{20}\text{E}_{20}$, and $\text{Gem}_{20}\text{E}_{30}$. Surfactants with smaller ethoxylation number in each series were found to be insoluble at room temperature.

D_2O was obtained from Aldrich (>99%). Solubility and cloud temperatures of 1 wt % solutions in D_2O and H_2O were measured by either visually observing or spectroscopically recording (at 500 nm with a UV–Vis spectrometer) the turbidity versus increasing temperature. The cloud temperature was taken to be the temperature where the solution first becomes significantly turbid.

Solutions for viscosity studies were prepared in water filtered through a Milli-Q purification system. Relative viscosities were measured using a capillary viscometer. The temperature was maintained to ± 0.1 °C in a water bath.

Small angle neutron scattering (SANS) was performed on the NG3 line at the Center for Neutron Research at NIST, Gaithersburg, Maryland. Neutrons with an average wavelength of 6.0 Å and a $\Delta\lambda/\lambda = 15\%$ were selected with a velocity selector. Scattering was from 1.0 mm path-length samples onto a 650×650 mm² 2D detector with 128×128 elements. The detector was offset by 0.2 m and scattering collected at two distances (1.4 and 13.1 m) giving a combined Q range of 0.0038 to 0.371 Å^{-1} . Raw SANS data was corrected for background, radially averaged and scaled to absolute intensity using standard procedures.¹³ Except where otherwise noted, data were fitted using the 1998 Igor routines provided by NIST.¹⁴

Results and Discussion

Dilute Solution Structure. Table 1 summarizes the solubilities and cloud temperatures for 1 wt % gemini solutions in H_2O and D_2O . Like conventional nonionic surfactants, the solubilities of these gemini surfactants in water are very sensitive to the alkyl and poly(oxyethylene) chain lengths.¹⁵ $\text{Gem}_{12}\text{E}_{10}$, $\text{Gem}_{14}\text{E}_{10}$, and

Table 1. Cloud Temperatures (°C) for 1 wt % Gemini Nonionic Surfactants with Different Hydrophobe Lengths (n) and Average Degrees of Ethoxylation (m) in D_2O and H_2O (in parentheses)

| n | m | | | |
|-----|----------|---------|-------|-------|
| | 10 | 15 | 20 | 30 |
| 12 | 59 (67) | > 100 | | |
| 14 | 46 (57) | > 100 | | |
| 20 | <i>a</i> | 81 (83) | > 100 | > 100 |

^a $\text{Gem}_{20}\text{E}_{10}$ is insoluble at room temperature, hence the cloud points could not be determined.⁴

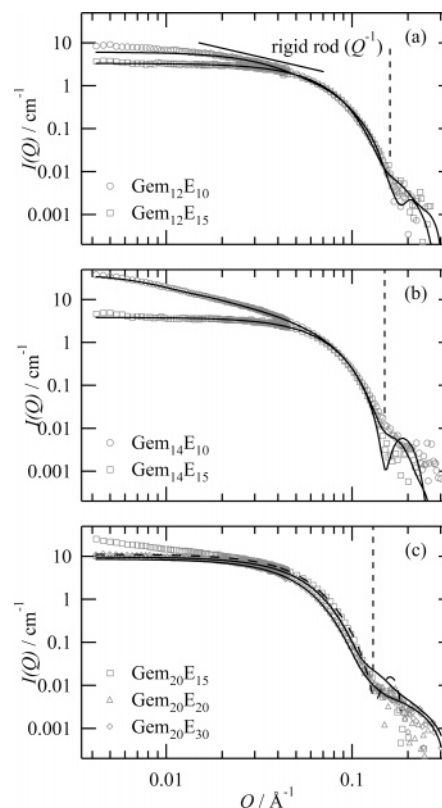


Figure 2. SANS spectra of 1 wt % solutions of $\text{Gem}_{12}\text{E}_m$ (a), $\text{Gem}_{14}\text{E}_m$ (b) and $\text{Gem}_{20}\text{E}_m$ (c) at 25 °C in D_2O showing fits to monodisperse core-shell spheres or rods (see Table 3). The solid line shows the Q^{-1} scattering behavior expected for long, rigid rodlike micelles.¹⁹

$\text{Gem}_{20}\text{E}_{15}$ all exhibit accessible cloud points on warming. $\text{Gem}_{12}\text{E}_{20}$, $\text{Gem}_{14}\text{E}_{20}$, $\text{Gem}_{20}\text{E}_{20}$, and $\text{Gem}_{20}\text{E}_{30}$ all have cloud temperatures above 100 °C in both H_2O and D_2O . The cloud point decreases with increasing alkyl chain length and increases with increasing degree of ethoxylation. The lowering of the cloud temperatures in D_2O relative to H_2O are similar to results reported previously for conventional nonionic surfactants.¹⁶

Figure 2 shows SANS spectra for all of the soluble gemini surfactants at 1 wt % and 25 °C. SANS spectra of micellar solutions are typically interpreted by separating the scattering into a form factor, $P(Q)$, describing scattering by individual micelles, and a structure factor, $S(Q)$, which is due to correlations between micelles arising from intermicellar interactions.¹⁷

(16) Zulauf, M.; Weckstrom, K.; Hayter, J. B.; Degiorgio, V.; Corti, M. *J. Phys. Chem.* **1985**, *89*, 3411–3417.

(17) Hayter, J. B. In *Physics of Amphiphiles: Micelles, Vesicles, and Microemulsions*; Degiorgio, V., Corti, M., Eds.; Elsevier Science: New York, 1983.

(7) Magid, L. J.; Triolo, R.; Johnson, J. S., Jr. *J. Phys. Chem.* **1984**, *88*, 5730–5734.

(8) Triolo, R.; Magid, L. J.; Johnson Jr, J. S.; Child, H. R. *J. Phys. Chem.* **1982**, *86*, 3689–3695.

(9) Lum Wan, J. A.; Warr, G. G.; White L. R.; Grieser, F. *Colloid Polym. Sci.* **1988**, *265*, 528–534.

(10) Mitchell, J. D.; Tiddy, G. J. T.; Waring, L.; Bostock, T.; McDonald, M. P. *J. Chem. Soc., Faraday Trans. 1* **1983**, *79*, 975–1000.

(11) Bernheim-Groszasser, A.; Tlustý, T.; Safran, S. A.; Talmon, Y. *Langmuir* **1999**, *15*, 5448–5453.

(12) Tlustý, T.; Safran, S. A.; Menes, R.; Strey, R. *Phys. Rev. Lett.* **1997**, *78*, 2616–2619.

(13) Lindner, P.; Zemb, T. N. *Neutron, X-Ray and Light Scattering: Introduction to an Investigative Tool for Colloid and Polymeric Systems*; North-Holland: Amsterdam, 1991.

(14) http://www.ncnr.nist.gov/programs/sans/manuals/data_anal.html (accessed 12/12/2004).

(15) Schick, M. J. In *Nonionic Surfactants*; Schick, M. J., Ed.; Marcel Dekker: New York, 1967.

$$I(Q) = (N_P \Delta \rho)^2 P(Q) S(Q)$$

where N_P is the number density of micelles, $\Delta \rho$ is the scattering contrast, and $Q = 4\pi/\lambda \sin(\theta)$, where 2θ is the scattering angle and λ is the neutron wavelength.

Separation into form and structure factors is only exact for monodisperse spheres but is often used as an approximation for polydisperse spheres or slightly elongated particles.¹⁷ It is certainly not valid for highly elongated micelles where interactions depend on orientation. For nonionic surfactants, we assume as a starting point that intermicellar interactions can be neglected at a concentration of 1 wt % ($S(Q) \rightarrow 1$),^{7,18} so that the scattering spectrum is described simply by considering $P(Q)$.

The radius of gyration, R_G , obtained from a series expansion of $P(Q)$ about $Q = 0$,^{20,21} of all the soluble gemini nonionics studied are listed in Table 2. In the absence of interactions, this gives a good overall measure of micelle dimensions independent of any assumptions about micelle shape. R_G may be compared with the radius of a spherical or cylindrical hydrocarbon core, which is upper bounded by the fully extended alkyl chain length of the surfactant: 16.7 Å for Gem₁₂, 19.2 Å for Gem₁₄, and 26.8 Å for Gem₂₀.⁶ In all cases, R_G is greater than expected for the core alone, and the results fall into two classes. Surfactants with longer ethylene oxide chains have radii of gyration around twice the expected core radius and are consistent with spherical micelles. These results compare well with reported radii of gyration for spherical micelles of C₁₂E₂₃ (Brij-35) of 30 Å²² and C₁₆E₂₀ (Brij-58) of 30.5 ± 0.6 Å.¹⁸ Those with the shortest ethylene oxide chains, Gem₁₂E₁₀, Gem₂₀E₁₅, and particularly Gem₁₄E₁₀, have much larger R_G suggesting instead eccentric or elongated micelles.

For homogeneous spheres, R_G can be used to obtain the overall sphere radius using $R_s = (5/3)^{1/2} R_G$.²³ However poly(oxyethylene) surfactants are known to form micelles with a hydrocarbon core and a corona or shell of hydrated ethylene oxide chains, which have different neutron scattering length densities.^{7,16} The core is usually regarded as homogeneous and hydrocarbon-like, whereas in the present systems the thickness of the surrounding ethylene oxide shell is comparable with the core radius and its scattering length density may vary radially.

SANS spectra of 1 wt % surfactant solutions in D₂O were fitted to core-shell sphere and rod structural models with pure (hydrogenous) hydrocarbon cores and a (D₂O) hydrated polyoxyethylene shell with a uniform scattering length density. In these surfactants with high degrees of ethoxylation, it is possible that the headgroups further from the core are more hydrated, so that the scattering length density of the shell increases from the hydrophobic core to the outer size of the micelle. To evaluate this effect, we compared the calculated scattering behavior for core-shell and core + ten-shell models with linearly varying scattering length density for the shell.¹⁷ The two scattering curves compare very well with each other and none of the main scattering features were significantly altered by the

Table 2. Radii of Gyration of Gemini Nonionic Surfactant Micelles in 1 wt % Solution at 25 °C

| surfactant | R_G (Å) |
|-----------------------------------|-----------|
| Gem ₁₂ E ₁₀ | 69 ± 5 |
| Gem ₁₂ E ₁₅ | 27 ± 3 |
| Gem ₁₄ E ₁₀ | 208 ± 20 |
| Gem ₁₄ E ₁₅ | 26 ± 6 |
| Gem ₂₀ E ₁₅ | 80 ± 50 |
| Gem ₂₀ E ₂₀ | 38 ± 3 |
| Gem ₂₀ E ₃₀ | 54 ± 5 |

increased number of fitting parameters.²⁴ This suggests that variations in scattering length density along the polyoxyethylene chains are not significant. Similarly, fitting the data to a "flower" model as used for star polymers^{25,26} did not indicate any hydrophilic chains extending far into solution, so we confined our analysis to a core + single shell model to describe micelle structure.

The independent fitted variables for core-shell spheres are the core radius (R_c) and the shell thickness ($t_{\text{shell}} = R_{\text{micelle}} - R_c$). The corresponding fitting parameters for core-shell rods are the cross-sectional radius of the core R_c , t_{shell} , and the length of the micelle core, L_c .

The other parameters required to describe the scattering functions are the number density of micelles, N_P , and the scattering length densities of the core, solvent and hydrated ethylene oxide shell, ρ_{core} , ρ_{solv} , ρ_{shell} , as well as the background coming from various sources such as incoherent scattering and ambient background. The total background, calculated using the Porod law,^{13,27,28} has been subtracted from all spectra. ρ_{core} was calculated from the scattering lengths and volumes of methyl and methylene fragments, and ρ_{solv} was taken as 1.914×10^{-4} Å³ for D₂O.^{17,29} ρ_{shell} is a volume weighted average of the scattering lengths of ethylene oxide fragments and D₂O

$$\rho_{\text{shell}} = \frac{\sum b_{\text{EO}} + (n_{\text{D}_2\text{O}}/m) \sum b_{\text{D}_2\text{O}}}{v_{\text{EO}} + (n_{\text{D}_2\text{O}}/m) v_{\text{D}_2\text{O}}}$$

where b_{EO} and $b_{\text{D}_2\text{O}}$ are the scattering lengths of an ethylene oxide unit (4.139×10^{-5} Å)^{17,29} and a D₂O molecule respectively, v_{EO} and $v_{\text{D}_2\text{O}}$ are the molecular volumes (calculated from known densities)³⁰ of an ethylene oxide unit (64.7 Å³) and a D₂O molecule, respectively. $n_{\text{D}_2\text{O}}/m$ is the ratio of D₂O molecules to ethylene oxide units in the headgroup region and was calculated from the shell volume, V_{shell}

$$n_{\text{D}_2\text{O}}/m = \frac{V_{\text{D}_2\text{O}}/v_{\text{D}_2\text{O}}}{m} = \left(\left(\frac{V_{\text{shell}}}{2mN_{\text{agg}}} \right) - v_{\text{EO}} \right) \frac{1}{v_{\text{D}_2\text{O}}} \quad (1)$$

where N_{agg} is the micelle aggregation number calculated by simply dividing the volume of the homogeneous micelle core, V_c , ($(4/3)\pi R_c^3$ for spheres; $\pi R_c^2 L$ for rods) by the volume of the hydrophobic moiety of a single molecule, v_{tail} , which here includes two alkyl chains and a hexamethylene spacer (864 Å³ for Gem₁₂; 972 Å³ for Gem₁₄; 1300 Å³ for Gem₂₀).²⁴

(18) Schefer, J.; McDaniel, R.; Schoenborn, B. P. *J. Phys. Chem.* **1988**, *92*, 729–732.

(19) de Gennes, P.-G. *Scaling Concepts in Polymer Physics*; Cornell University Press: Ithaca, NY, 1979.

(20) Guinier, A.; Fournet, G. *Small-Angle Scattering of X-rays*; John Wiley and Sons: New York, 1955.

(21) Zimm, B. H. *J. Chem. Phys.* **1948**, *16*, 1093–1099.

(22) Preu, H.; Zradba, A.; Rast, S.; Kunz, W.; Hardy, E. H.; Zeidler, M. D. *Phys. Chem. Chem. Phys.* **1999**, *1*, 3321–3329.

(23) Glatter, O.; Kratky, O. *Small-Angle X-ray Scattering*; Academic Press: New York, 1982.

(24) FitzGerald, P., Ph.D. Thesis, University of Sydney, Sydney, Australia, 2002. Available from The Australian Digital Thesis Program <http://adt.caul.edu.au/> (accessed 12/12/2004).

(25) Richetti P. Personal communication.

(26) Daoud, M.; Cotton J. P. *J. Phys. (Paris)* **1982**, *43*, 531–538.

(27) Porod, G. *Kolloid-Z.* **1951**, *124*, 83–114.

(28) Porod, G. *Kolloid-Z.* **1952**, *125*, 51–57.

(29) Sears, V. F. *Neutron News* **1992**, *2*, 26–37.

(30) *CRC Handbook of Chemistry and Physics*; CRC Press: Cleveland, Ohio, 1977.

Table 3. Best Fit Parameters for 1 wt % Gemini Surfactants at 25 °C (Figure 2) Showing the Model that Yielded the Best Fit^a

| surfactant | model | R_c (Å) | t_{shell} (Å) | R_{tot} (Å) | L_c (Å) | ρ_{shell} ($\times 10^{-6}$ Å ⁻²) | n_{D_2O}/m | N_{agg} | t_{calc} (Å) | R_F (Å) |
|-----------------------------------|--------|-----------|------------------------|----------------------|-----------|--|--------------|------------------|-----------------------|-----------|
| Gem ₁₂ E ₁₀ | rod | 13 | 20 | 33 | 130 | 4.6 | 4.8 | 79.9 | 12.3 | 14.9 |
| Gem ₁₂ E ₁₅ | sphere | 17.8 | 21.2 | 39.0 | | 5.0 | 6.8 | 27.3 | 16.2 | 18.9 |
| Gem ₁₄ E ₁₀ | rod | 14.8 | 18.2 | 33.0 | 650 | 3.7 | 2.5 | 460 | 12.5 | 14.9 |
| Gem ₁₄ E ₁₅ | sphere | 19.2 | 20.5 | 39.7 | | 4.9 | 6.2 | 30.5 | 15.8 | 18.9 |
| Gem ₂₀ E ₁₅ | rod | 19 | 18 | 37 | <i>b</i> | 4.1 | 3.4 | <i>b</i> | 18.2 | 18.9 |
| Gem ₂₀ E ₂₀ | sphere | 26.0 | 26.1 | 52.1 | | 5.2 | 8.3 | 56.8 | 20.9 | 22.4 |
| Gem ₂₀ E ₃₀ | sphere | 22.8 | 29.9 | 52.7 | | 5.6 | 13.7 | 39.3 | 27.8 | 28.3 |

^a R_c is the radius of the hydrocarbon core of the micelle, t_{shell} is the thickness of the polyoxyethylene shell, R_{tot} is the total radius ($R_c + t_{\text{shell}}$), L_c is the core length of a core-shell rod (the total length is $L_c + 2t_{\text{shell}}$), ρ_{shell} is the scattering length density of the shell obtained from n_{D_2O}/m , t_{calc} is the thickness of the polyoxyethylene layer calculated from scaling arguments, and R_F is the Flory radius (see text).
^b The fitted length of the core was 131 Å and aggregation number 115; however, due to the poor quality of the fit at low Q , this should only be taken to indicate an anisotropic micelle.

The number density of micelles (micelles divided by volume) was calculated from

$$N_p = \frac{\phi_{\text{HC}}}{V_c}$$

where ϕ_{HC} is the volume fraction of hydrocarbon from²⁴

$$\phi_{\text{HC}} = \frac{\frac{\phi_{\text{m,HC}}}{d_{\text{HC}}}}{\frac{\phi_{\text{m,HC}}}{d_{\text{HC}}} + \frac{\phi_{\text{m,EO}}}{d_{\text{EO}}} + \frac{\phi_{\text{m,solv}}}{d_{\text{solv}}}}$$

where $\phi_{\text{m,HC}}$, $\phi_{\text{m,EO}}$, and $\phi_{\text{m,solv}}$ are the mass fractions of hydrocarbon tails, ethylene oxide and D₂O respectively, and d_{HC} , d_{EO} , and d_{solv} are the corresponding densities (assumed to be the same as the bulk densities). The mass fractions were calculated from

$$\phi_{\text{m,HC}} = \phi_{\text{m,surfactant}} \frac{\text{Mw}_{\text{tail}}}{\text{Mw}_{\text{surf}}}$$

$$\phi_{\text{m,EO}} = \phi_{\text{m,surfactant}} \frac{\text{Mw}_{\text{head groups}}}{\text{Mw}_{\text{surf}}}$$

$$\phi_{\text{m,solv}} = 1 - (\phi_{\text{m,HC}} + \phi_{\text{m,EO}})$$

where $\phi_{\text{m,surfactant}}$ is the mass fraction of surfactant in solution and Mw_{tail} , $\text{Mw}_{\text{headgroups}}$, and Mw_{surf} are the molecular weights of the tail, the combined headgroups and the total surfactant.

Figure 2 shows the best fits of monodisperse core-shell models to the SANS spectra of 1 wt % gemini nonionic surfactants at 25 °C, with corresponding values of the various fitted parameters listed in Table 3. Like conventional nonionic surfactants, these gemini surfactants form spherical micelles for the largest headgroups and rodlike micelles for the smallest headgroups. Good fits are obtained over the entire Q range examined to the core-shell sphere model for Gem₁₂E₁₅, Gem₁₄E₁₅, and Gem₂₀E₂₀, and to the core-shell rod model for Gem₁₄E₁₀. The scattered intensity from Gem₁₄E₁₀ clearly shows expected Q^{-1} decay at low Q for long, rigid rods,¹⁹ consistent with its large R_G (Table 2). Gem₂₀E₃₀ is well described by a core-shell sphere model at high Q , but also has higher than expected scattering at low Q (Figure 2c).

Gem₁₂E₁₀ and Gem₂₀E₁₅ are best fitted as short core-shell rods, but no simple shape yielded a good fit over the entire Q range. For both of these systems, the experimental scattered intensity is higher than predicted by the model at low Q , and the fit might be improved by including

additional structural features such as spherical end caps on the micelles, flexibility in the rods, or micelle polydispersity. Intermicellar attractions could also be responsible for the discrepancy; however, these are probably not significant as an adequate fit was obtained for the much longer rods of Gem₁₄E₁₀ and for Gem₂₀E₁₅ at higher temperatures, as discussed below.

Considering first the spherical micelles formed by Gem₁₂E₁₅, Gem₁₄E₁₅, and Gem₂₀E₂₀, the fitted hydrocarbon core radii of 17.8, 19.2, and 26 Å are in good agreement with the expected fully extended alkyl chain lengths, l_c , of 16.7, 19.2, and 26.8 Å.⁶ The micelle core is consistent with the standard picture for conventional surfactants, although the radius may be slightly greater than expected for Gem₁₂E₁₅ because of the hexamethylene spacer.

The core radius of the rodlike micelles is in every case notably smaller than the corresponding spheres, with 13 Å versus 17.8 Å for Gem₁₂E₁₀, 14.8 Å versus 19.2 Å for Gem₁₄E₁₀, and 19 Å versus 23–26 Å for Gem₂₀E₁₀. This has also been observed previously for conventional surfactants³¹ and can be understood qualitatively by considering the thermodynamics of rodlike micelles. Israelachvili et al.⁵ have argued that rodlike micelles form spherical end caps in order to reduce the free energy cost of hydrocarbon ends in contact with water. Using a combination of thermodynamic and geometric arguments, they show that the ratio of the area of the rod (a_o) to the area of the end caps (a) lies between 2/3 and 1. From this expression, it can be shown that the cross-sectional radius of the rod must lie between $2l_c/3$ and l_c , which forms an upper bound on the radius of a spherical section end-cap. That is, the radius of a rodlike micelle will be up to 1/3 less than that of a sphere, which is close to the radius ratio observed here.

Among the rod-forming micelles, the fitted length of the cores increases significantly as alkyl tail length is increased from Gem₁₂E₁₀ to Gem₁₄E₁₀. The micelle sphere-to-rod transition is very sensitive to alkyl chain length in both ionic and nonionic conventional surfactants.³² Here too a small change in chain length produces a large effect. It has been conjectured previously that longer alkyl chains may not be fully extended in the micelle core.³³ In the language of the surfactant packing parameter, this means that alkyl chain volume, v , increases faster than the micelle radius, which is less than l_c , leading to a lower curvature. Our results showing the smaller radii of the hydrocarbon core of rodlike micelles also support this proposition.

(31) Glatter, O.; Fritz, G.; Lindner, H.; Brunner-Popela, J.; Mittelbach, R.; Strey, R.; Egelhaaf, S. U. *Langmuir* **2000**, *16*, 8692–8701.

(32) Rehage, H.; Hoffmann, H. *Faraday Discuss. Chem. Soc.* **1983**, *76*, 363–373.

(33) Blackmore, E. S.; Tiddy, G. J. T. *J. Chem. Soc., Faraday Trans. 2* **1988**, *84*, 1115–1127.

Micelle aggregation numbers, N_{agg} , are shown in Table 3. Like the hydrocarbon core radii, the aggregation numbers for Gem₁₂E₁₅, Gem₁₄E₁₅, and Gem₂₀E₂₀ agree well with expectations for spherical micelles with fully extended alkyl chains (i.e., a surfactant packing parameter of exactly one-third). However, both the radius and aggregation numbers of Gem₂₀E₃₀ are smaller than expected, and this is considered below.

The corona of polyoxyethylene chains behaves as a fairly homogeneous layer with an approximately constant scattering length density. The fitted shell thickness of 20–30 Å is comparable with or greater than the corresponding hydrophobic core radii, making these micelles somewhat similar to those formed by block copolymers. Considering first only spherical micelles, the shell thickness increases with increasing polyoxyethylene chain length. These results are also consistent with recent results for C₁₂E₂₃ micelles, which yielded a core radius of 15–17 Å and a homogeneous shell thickness of approximately 25 Å,²² close to the value we obtain for Gem₂₀E₂₀.

The measured shell thickness is much smaller than the fully extended (all trans) lengths of approximately 40 Å for E₁₀ or 120 Å for E₃₀ and is consistent with the polyoxyethylene chains adopting a coiled conformation in aqueous solution. The conformation of polyoxyethylene chains and the structure of the hydrophilic shell in nonionic surfactant micelles has long been a subject of investigation.^{7,15,34,35} The characteristic dimension of a polyoxyethylene coil of m units in water can be described by its end-to-end distance or Flory radius, $R_F = lm^\alpha$, where the statistical segment length of CH₂CH₂O is $l = 3.9$ Å and the exponent $\alpha = 0.583$.³⁶ However, polymer chains tethered on a surface may be extended into a brush-like conformation by excluded volume interactions with their neighbors. Johnsson et al.³⁷ have recently used such a model, developed for much longer starlike block copolymer micelles, to describe polyoxyethylene chains as short as 17 units in the corona of spherical lipid micelles. The shell thickness around a sphere in this model is given by³⁸

$$t_{\text{calc}}(\text{sphere}) = \left[ml^{1/\alpha} \frac{8N_{\text{chain}}^{(1-\alpha)/2\alpha}}{3\alpha 4^{1/\alpha}} - R_c^{1/\alpha} \right]^\alpha - R_c \quad (2)$$

where N_{chain} is the number of chains attached to the micelle surface, here twice the micelle aggregation number.

The same scaling arguments can be applied to describe the conformation of chains tethered to a rodlike micelle, yielding

$$t_{\text{calc}}(\text{rod}) = \left[m \frac{1 + \alpha}{3\alpha} l^{1/\alpha} \left(\frac{\pi R_c^2}{4v} \right)^{(1-\alpha)/2\alpha} - R_c^{(1+\alpha)/2\alpha} \right]^{2\alpha/(1+\alpha)} - R_c \quad (3)$$

Here v is the volume occupied by one gemini surfactant in the hydrophobic core. Thus, $2\pi R_c^2/v$ is equal to the number of tethered polyoxyethylene chains (2 per molecule) per unit of length along the core, N_{chain}/L_c .

Shell thicknesses for spheres and rods, t_{calc} , calculated in this way using best-fit core radii are listed in Table 3.

(34) Röscher, M. In *Nonionic Surfactants*; Schick, M. J., Ed.; Marcel Dekker: New York, 1967.

(35) Tanford, C.; Nozaki, Y.; Rohde, M. F. *J. Phys. Chem.* **1977**, *81*, 1555–1560.

(36) Devanand, K.; Selser, J. C. *Macromolecules* **1991**, *24*, 5943–5947.

(37) Johnsson, M.; Hansson, P.; Edwards, K. *J. Phys. Chem. B* **2001**, *105*, 8420–8430.

(38) Vagberg, L. J. M.; Cogan, K. A.; Gast A. P. *Macromolecules* **1991**, *24*, 1670–1677.

In every case except Gem₂₀E₁₅, the calculated thickness is less than the experimentally fitted shell thickness. More remarkably, it is in every case less than the unperturbed Flory radius of the polyoxyethylene chain, R_F . (The same is true for the results of Johnsson et al.,³⁷ for which the layer thickness only exceeds R_F for chains containing more than 80 ethoxy units.) This suggests that tethering to a hydrophobic core alone does not lead to stretching of these shorter chains. Rather, at least within this model, the curvature of the interface and low attachment density allows them to extend laterally even more than in bulk solution.

Experimental shell thicknesses are on average 2.4 Å thicker than the unperturbed chain dimension, R_F . Although less than the length of a single ethoxy unit, this small difference is uniformly observed and is especially apparent if only spherical micelles are considered. This may arise from some chain extension or preferential orientation of ethoxy segments near the hydrophobic core. However, these surfactants are polydisperse in their polyoxyethylene chains, so that 50% of chains are longer than the average degree of ethoxylation. For example, the experimentally measured thickness of 21.2 Å for Gem₁₂E₁₅ corresponds to R_F of the 75th percentile of the chain distribution and 24.1 Å to the 90th percentile. This would also be more than enough to account for the discrepancy between measured and predicted shell thickness for all of the surfactants studied.

This finally leaves us with a picture of a polyoxyethylene shell around spherical or elongated micelles consisting of chains in conformations close to their unperturbed solution dimensions. No gradient in composition is or should be needed to describe the structure of the shell.

The amount of water per ethoxy monomer unit in the shell, $n_{\text{D}_2\text{O}}/m$, is obtained from the fitted data using eq 1. All of the values obtained are much larger than the 1.2–2.0 $n_{\text{D}_2\text{O}}/m$ values typically obtained for conventional nonionic surfactants with smaller polyoxyethylene chains^{7,17} but compares well with a value of around 7 obtained for C₁₂E₂₃.²² The results are in fact consistent with the available volume for D₂O inside a polyoxyethylene coil of m units, which may be estimated by subtracting the volume occupied by the chain monomers from the total volume of the (unstretched) coil

$$V_{\text{D}_2\text{O}} = \frac{\pi}{6} R_F^3 - mv_{\text{EO}} = \frac{\pi}{6} l^3 m^{3\alpha} - mv_{\text{EO}} \quad (4)$$

The number of D₂O molecules that can be accommodated per ethoxy unit within the coil is then just

$$n_{\text{D}_2\text{O}}/m = \frac{V_{\text{D}_2\text{O}}/v_{\text{D}_2\text{O}}}{m} = \frac{\frac{\pi}{6} l^3 m^{3\alpha-1} - v_{\text{EO}}}{v_{\text{D}_2\text{O}}} \quad (5)$$

which increases as $m^{0.75-0.8}$ for a polymer chain in a good solvent like polyoxyethylene in water. The values and trends in the water-to-ethoxy ratios and corresponding shell scattering length densities thus calculated agree well with the fitted data, as listed in Table 4. These values thus simply reflect the fact that shell scattering includes all of the water present, not only water of solvation, and that the amount of available volume for solvent increases with chain length.

We return briefly to the low aggregation number obtained for Gem₂₀E₃₀ (Table 3). The smaller core is very likely to be an accommodation by the hydrophobic chains

Table 4. Calculated and Fitted Parameters for Polyoxyethylene Shells of Gemini Nonionic Surfactants

| M | n_{D2O}/m calc. | n_{D2O}/m expt. | ρ_{shell} ($\times 10^{-6} \text{ \AA}^{-2}$) calc. | ρ_{shell} ($\times 10^{-6} \text{ \AA}^{-2}$) expt. |
|-----------------|----------------------|----------------------|--|--|
| 10 ^a | 3.7 | 2.5, 4.8 | 4.2 | 3.7, 4.6 |
| 15 ^a | 5.7 | 3.3, 6.2, 6.8 | 4.8 | 4.1, 4.9, 5.0 |
| 20 | 7.6 | 8.3 | 5.1 | 5.2 |
| 30 | 11.1 | 13.7 | 5.4 | 5.6 |

^a Multiple values correspond to different alkyl chain lengths with the same degree of ethoxylation, m ; Gem₁₂E₁₀, Gem₁₄E₁₀; Gem₁₂E₁₅, Gem₁₄E₁₅, Gem₂₀E₁₅.

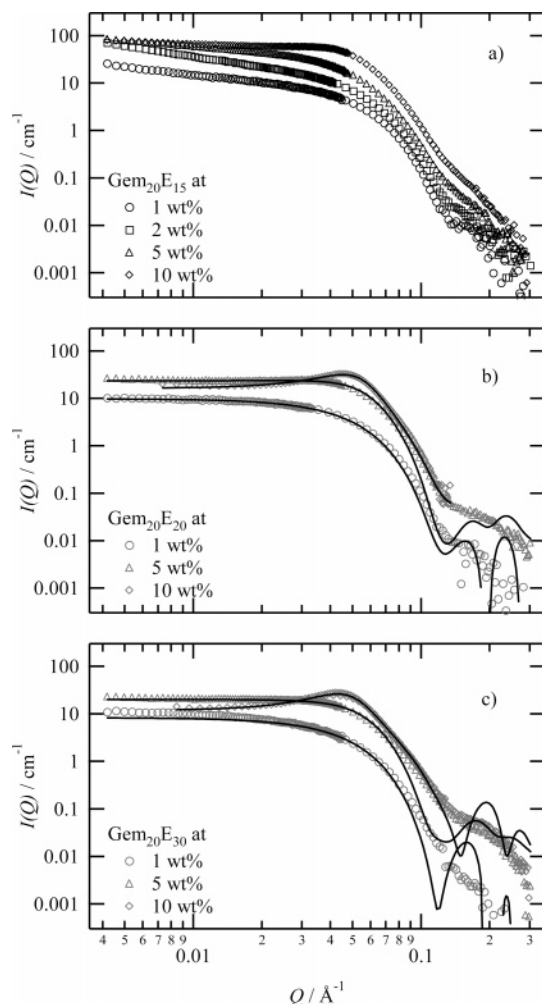


Figure 3. SANS spectra for (a) Gem₂₀E₁₅, (b) Gem₂₀E₂₀, and (c) Gem₂₀E₃₀ at 1 wt % (circles), 2 wt % (squares), 5 wt % (triangles), and 10 wt % (diamonds). Hard sphere fits are shown for Gem₂₀E₂₀ and Gem₂₀E₃₀ (see Table 5 for best fit values).

of the conformation adopted by the larger E₃₀ chain in water, similar to effects seen in block copolymer micelles.³⁹

Concentrated Solutions. Figure 3 shows SANS spectra for solutions of Gem₂₀E₁₅, Gem₂₀E₂₀, and Gem₂₀E₃₀ respectively at concentrations between 1 and 10 wt %. SANS spectra for Gem₂₀E₂₀ and Gem₂₀E₃₀, which form spherical micelles in dilute solution, were fitted using a core-shell form factor¹⁷ together with a hard sphere structure factor (using the Percus–Yevick closure).⁴⁰ The fitting parameters are the same as in the dilute solution case, together with an effective hard-sphere volume

Table 5. Best Fit Values for Gem₂₀E₂₀ and Gem₂₀E₃₀ at 1, 5, and 10 wt %^a

| surfactant | ϕ_{HS} | R_c (\AA) | t_{shell} (\AA) | p | ρ_{shell} ($\times 10^{-6} \text{ \AA}^{-2}$) |
|-----------------------------------|-------------|---------------------------|---------------------------------|------|---|
| Gem ₂₀ E ₂₀ | | | | | |
| 1 wt % | | 26.0 | 26.1 | | 5.2 |
| 5 wt % | 0.11 | 25.4 | 23.2 | 0.09 | 3.9 |
| 10 wt % | 0.21 | 31.3 | 24.0 | 0.07 | 5.1 |
| Gem ₂₀ E ₃₀ | | | | | |
| 1 wt % | | 22.8 | 29.9 | | 5.6 |
| 5 wt % | 0.084 | 21.1 | 26.5 | 0.12 | 3.7 |
| 10 wt % | 0.21 | 32.0 | 28.1 | 0.00 | 5.5 |

^a ϕ_{HS} is the effective hard sphere volume fraction of interacting micelles, R_c is the core radius, t_{shell} is the shell thickness, p is the polydispersity (the variance divided by the mean radius), ρ_{shell} is the scattering length density of the shell.

fraction of micelles, which determines $S(Q)$. Best fits are shown in Figure 3 and fitting parameter values are given in Table 5. The model used here also allows for some polydispersity in the micelle sizes. We found this to be smaller in every case than the smearing due to the 15% wavelength spread in the incident neutrons and so has been disregarded.

This model fits the experimental data well at low Q and near the peak for both Gem₂₀E₂₀ and Gem₂₀E₃₀, as expected for interacting spherical micelles. The fits are poorer at higher Q , where they fall away from the peak too sharply. This is probably because the micelles do not interact as hard spheres but via a soft steric repulsion between ethylene oxide headgroups. For further details, see ref 24.

This is also evident from the effective hard sphere volume fractions of the micelles, which are roughly double the real volume fractions. True volume and weight fractions should be approximately the same in these systems because the densities of the surfactant and the solvent are almost the same. This artifact arises from the large volume of water in the polyoxyethylene shell, discussed above, which increases the effective volume fraction of the micelles and in turn produces the steeper falloff in intensity at high Q in the hard-sphere model. The volume fraction of micelles including all water in the shell is expected to be 3.3–3.6 times greater than the dry volume fraction, whereas the best fit data yields only about 2. Micelle structural parameters, R_c , t_{shell} , and especially ρ_{shell} , do not vary systematically with surfactant concentration, so we conclude that the micelle sizes do not change very much in the range examined. The observed variations probably arise simply from inconsistencies in modeling the polyoxyethylene shell in the form and structure factors, and should not be over interpreted.

The nearest neighbor center-to-center distance (D) estimated from the peak position using¹³ $D = 2\pi/Q_{peak}$ yields $D \sim 140 \text{ \AA}$ for Gem₂₀E₂₀ and $D \sim 150 \text{ \AA}$ for Gem₂₀E₃₀ at 10 wt %. These values are comparable with the fitted micelle diameters of 105–110 and 110–120 \AA , respectively, again underscoring the problems associated with a hard-sphere interaction in these systems.

Effects of Temperature. Figure 4 shows SANS spectra for 1 wt % solutions of Gem₁₂E₁₀, Gem₁₄E₁₀, and Gem₂₀E₁₅ as a function of temperature from 20 $^{\circ}\text{C}$ up toward their respective cloud points. All three show an increase in the scattering at low Q indicating the formation and growth of cylindrical micelles. Both Gem₁₄E₁₀ and Gem₂₀E₁₅ already form elongated micelles at 20 $^{\circ}\text{C}$. Only Gem₁₂E₁₀ shows the complete evolution from near-spherical or short rodlike micelles at 20 $^{\circ}\text{C}$ into the Q^{-1} dependence expected for long, rigid rods.¹⁹ For each of these surfactants, the

(39) Halperin, A. *Macromolecules* **1987**, *20*, 2943–2946.

(40) Percus, J. K.; Yevick, G. J. *Phys. Rev.* **1958**, *110*, 1–13.

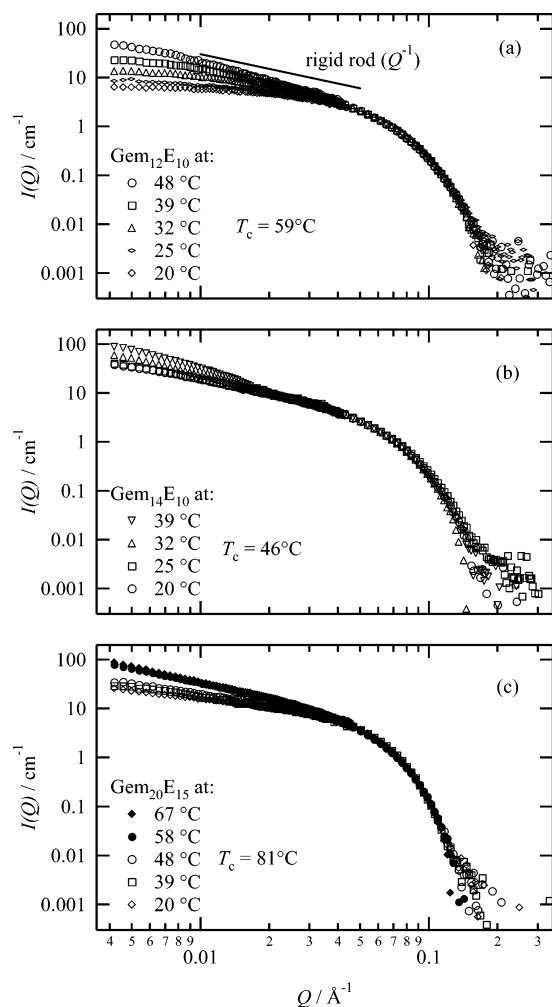


Figure 4. SANS spectra as a function of temperature for 1 wt % solutions of (a) Gem₁₂E₁₀, (b) Gem₁₄E₁₀, and (c) Gem₂₀E₁₅ in D₂O. T_c is the cloud temperature for each surfactant in D₂O (see Table 1).

SANS data indicates elongation at low temperatures before approaching a Q^{-1} dependence several degrees below the cloud temperature, i.e., short rigid rodlike micelles¹⁹ that grow as the cloud temperature is approached.

The shape of nonionic micelles as a function of temperature has long been studied using SANS. Zulauf et al. found increased scattering by C₈E₄,⁴¹ C₈E₅,^{16,17,41} and C₁₂E₈,¹⁶ solutions at low Q with increasing temperature, which they interpreted as attractions between spherical micelles. They proposed that the micelles form loose "clouds" due to a short-range attraction that became stronger as the temperature approached the cloud point. Triolo et al., studying C₁₂E₆⁸ and C₁₂E₈,⁷ found a similar scattering behavior and attributed it to critical concentration fluctuations between spherical micelles. However, Lum Wan et al.⁹ have shown (for C₁₂E₆ at least) that these data could also be interpreted as polydisperse, rodlike micelles, and that SANS, in isolation of other techniques, is not capable of distinguishing between the two models.

More recently, Glatter et al.³¹ have studied C₈E_{3,4,5}, C₁₀E₄, and C₁₂E_{5,6} from 3 °C up to their cloud temperatures with a combination of SANS and viscosity measurements. Using a more complex method^{42,43} than previous studies, they interpreted the solution structure as interacting,

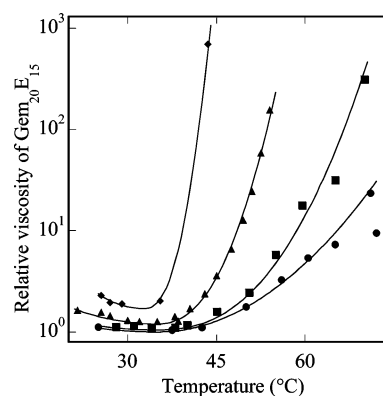


Figure 5. Relative viscosity as a function of temperature for Gem₂₀E₁₅ at 1 wt % (●), 2 wt % (■), 5 wt % (▲), and 10 wt % (◆). Solid lines are guides to the eye.

rodlike micelles, finding a sphere-to-rod transition with increasing temperature. Further, surfactants with small headgroups, such as C₈E₄ ($T_c \sim 37$ °C) and C₁₂E₅ ($T_c \sim 30$ °C), formed rodlike micelles even at low temperatures.

The general trends obtained here for the gemini surfactants compare well with the study by Glatter et al.³¹ Surfactants with small headgroups form rodlike micelles at low temperatures, whereas larger headgroups produce spherical micelles. As the cloud temperature is approached, the micelles undergo a sphere-to-rod transition and micellar growth.

The viscosity of Gem₂₀E₁₅ also strongly suggests a sphere-to-rod transition on warming. Figure 5 shows the temperature dependence of the relative viscosity of Gem₂₀E₁₅ aqueous solutions. Below about 40 °C, the solutions are Newtonian and have low viscosities, but on warming, the viscosity increases rapidly at all concentrations studied. At 1 wt %, η_r increases by a factor of about 10 between 40 and 70 °C. At 10 wt %, the sample was visually observed to become viscoelastic at approximately 50 °C and then gelled near 60 °C so that no flow was observed in the viscometer. The massive increase in viscosity above 40 °C corresponds well with the large increase in low angle scattering and supports the growth of rigid rodlike micelles and formation of an entangled network.

No such effects of temperature on viscosity increases were observed for the shorter tailed Gem₁₂E₁₀, and only a slight increase in viscosity occurred for Gem₁₄E₁₀ just below the cloud temperature, despite both approaching a Q^{-1} scattering dependence. We conclude therefore that the high viscosity is a consequence of the higher energies required for scission of rodlike micelles with two C₂₀ alkyl chains ($R_c = 19$ Å) compared with C₁₂ or C₁₄ ($R_c = 13$ or 15 Å). A similar dependence of viscosity (and viscoelasticity) on alkyl chain length has been observed for elongated micelles of the well-known alkyltrimethylammonium salicylate surfactants.³² For 1 mM solutions, the viscosity was found to increase by a factor of 10 when the alkyl chain was increased from C₁₂ to C₁₄ but by a factor of 100 when further increased to C₁₆.

Conclusions

The structure of aqueous Gem_{*n*}E_{*m*} micelles is similar to that of conventional, or monomeric nonionic surfactants.

(42) Brunner-Popela, J.; Glatter, O. *J. Appl. Crystallogr.* **1997**, *30*, 431–442.

(43) Weyerich, B.; Brunner-Popela, J.; Glatter, O. *J. Appl. Crystallogr.* **1999**, *32*, 197–209.

(41) Zulauf, M.; Rosenbusch, J. P. *J. Phys. Chem.* **1983**, *87*, 856–862.

The presence of two alkyl chains and a hexamethylene spacer decreases their solubility, so that longer polyoxyethylene chains are needed on each alkyl tail to confer solubility, but after this the trends on behavior are familiar. At room-temperature Gem₁₂E₁₅, Gem₁₄E₁₅, Gem₂₀E₂₀, and Gem₂₀E₃₀ all form spherical micelles; Gem₂₀E₁₅ and Gem₁₂E₁₀ form slightly anisotropic (short rod) micelles, whereas Gem₁₄E₁₀ (which has the largest packing parameter value among the surfactants examined) forms long rodlike micelles. Increasing the temperature of the Gem₁₂E₁₀, Gem₁₄E₁₀, and Gem₂₀E₁₅ from 20 °C toward their cloud temperature results in the growth of long rodlike micelles. In Gem₂₀E₁₅, this is accompanied by a marked increase in viscosity, the onset of viscoelasticity at low concentrations, and gelation of the solution at higher concentrations. Such an effect has not previously been reported for nonionic surfactants to our knowledge.

The polyoxyethylene chains in the micelle corona are well-described by a random coil chain in a good solvent

having an approximately constant composition and scattering length density, with no significant chain stretching as occurs for longer chains and for star polymers.

Acknowledgment. This work was supported by the Australian Research Council Industry Linkage Program, Orica Australia, and Huntsman Chemicals. P.A.F. acknowledges receipt of an ARC postgraduate scholarship, and T.W.D. acknowledges receipt of a Henry Bertie and Florence Mabel Gritton Postdoctoral Fellowship from the University of Sydney. This work utilized facilities supported in part by the National Science Foundation under Agreement No. DMR-9986442. We acknowledge the support of the National Institute of Standards and Technology, U.S. Department of Commerce, in providing the neutron research facilities used in this work.

LA0467988